PERFORMANCE OF A LARGE VACUUM FACILITY FOR SPACECRAFT PROPULSION TESTING

F. Scortecci[1], E. Bonelli[1], B. Michelozzi[1], F. Saito[2], S. Scaranzin[1], A. Turco[1]

[1]*AEROSPAZIO Tecnologie s.r.l., Rapolano Terme, Siena, Italy, Email: aerospazio@aerospazio.com*
[2] *Department of Information Engineering, Siena, Italy*

ABSTRACT

A Large Vacuum Test Facility has been developed at AEROSPAZIO Tecnologie with the aim of providing high qualified test services in Electric Propulsion and Space Simulation. The test facility consist of a stainless steel cylinder 3.8 m diameter and 11.5 m overall length. A modular cryopumping system allows 200.000 l/s continuous pumping speed of Xe. Beam diagnostics, including Faraday probes and Retarding Potential Analysers, have been installed. A test campaign aimed at evaluating the EMC characteristics of the test site has been performed.

1. INTRODUCTION

The implementation of any new technology in the satellite market requires a careful understanding not only on the performance, but also on the integration issues. In this regard, Electric Propulsion, especially of high power, requires a particular extensive investigation due to the complex phenomena that occur on the fully deployed satellite. It is evident that the industrial development of high power electric thrusters rely on the availability of suitable test facilities where on-orbit operations can be simulated with reliability.

Therefore, a Large Vacuum Test Facility has been developed at AEROSPAZIO so as to allow high fidelity characterization of high power Xenon electric thrusters.

2. THE VACUUM FACILITY

The Large Vacuum Test Facility (LVTF) located at AEROSPAZIO (Fig. 1) consists of a horizontal stainless steel cylinder with two full diameter end caps, which can be removed to allow the introduction of large test articles. The chamber is 11.5 m long and has a diameter of 3.8 m for a total volume of 120 m^3. On the side of the chamber there are three 900 mm diameter flanges which allow connecting through gate valves up to three service chambers for parallel tests of several articles.

To date, the following pumps are installed on the chamber (Fig. 2):

- a 1st stage consisting of a roots blower (1200 m^3/h pumping speed) backed by a rotary pump;

Fig. 1. The Large Vacuum Test Facility.

- a 2nd stage consisting of a turbomolecular pump (1000 l/s pumping speed) backed by a dry rotary pump;
- a 3rd stage consisting of two cryopumps (20.000 l/s pumping speed);
- a 4th stage consisting of a special system of panels cryocooled by Cold Heads and Liquid Nitrogen baffles, specifically designed to pump Xenon.
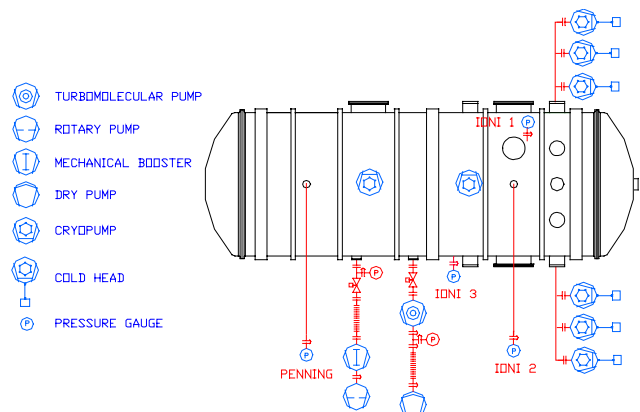

Fig. 2. The vacuum pumps system.

Vacuum diagnostics include one Penning and three combined full range gauges (a Pirani 1st stage and a Bayard Alpert hot cathode 2nd stage) placed at several

locations in the chamber. Several Pirani gauges are used to monitor the pressure in different places of the lines during the pumpdown phases.

Gauges are factory calibrated for Nitrogen. No additional calibrations were performed in situ. Therefore, the accuracy reported in Tab. 1 is assumed after 5 min from switching-on.

Tab. 1. Accuracy of the pressure gauge.

Gauge	Accuracy (% of the readings)	Range (mbar)
Pirani	15	$100 - 1 \times 10^{-3}$
Penning	30	$1 \times 10^{-2} - 1 \times 10^{-8}$
Ionisation	15	$1 \times 10^{-4} - 1 \times 10^{-8}$

The real vacuum conditions during thruster operations (corrected measurements) are obtained by dividing the gauge outputs (uncorrected measurement) by the Xe gas correction factor 2.87.

All facility pressures and operating parameters are acquired and stored by the Test Facility Data Acquisition System (DAS).

The DAS hardware is based on a PC architecture:
- National Instruments® DAQ card multiplexed and conditioned by a SCXI system;
- 64 single ended or 32 differential channels, 200 kS/s max sampling rate;
- 12 bit A/D converter;
- gain selectable from 1 to 2000.

The DAS software was developed by AEROSPAZIO in collaboration with the Dept. of Information Eng. of the University of Siena [1].

The Facility Management System (FMS) consist of several digital I/O cards, the control electronics and the software for management and control.

The FMS monitors the state of the pumping system, allows the remote operation of the valves and pumps and shows the data acquired by the DAS, storing all the events in a log file. Major equipment malfunctions and/or facility shut down result in immediate safety reaction operations and a corresponding visual and acoustic notification to aid and preventing damage to the facility or to the test hardware.

3. TEST ARRANGEMENTS

A water cooled beam target is mounted at the chamber end opposite w.r.t. the cryogenic system (Fig. 3). The target is covered with pure graphite plates to minimise sputtering toward the thruster. The interior of the test facility is also fully lined with pure graphite panels.

To date, two thruster position along the chamber axis can be chosen:
- station 1: in front of the cryopanels, 7.5 m from the beam target, $\sim$80 m^3 of free firing volume;
- station 2: behind the cryopanels, >10 m from the beam target, $\sim$108 m^3 of free firing volume.

The high vacuum gauges are located on the chamber at the following axial distances from the thruster station 1:

	Ioni 1	Ioni 2	Ioni 3	Penning
Axial Distance (m)	0	0.6	1.8	5.8

A rotating semicircular boom is installed inside the chamber so as to describe a hemisphere with a radius of 1 m, in front of the thruster station 1. The beam diagnostics mounted on the boom include Faraday Probes and Retarding Potential Analysers (Par. 5).

The boom is moved by a stepper motor with a step angle of 0.45 deg and can perform a 160 deg rotation (-70 deg to +90 deg off axis). The stepper motor is controlled by a PC based system.

The angular position accuracy of the probes is less than 0.5 deg, the radial distance accuracy less than 0.1%.
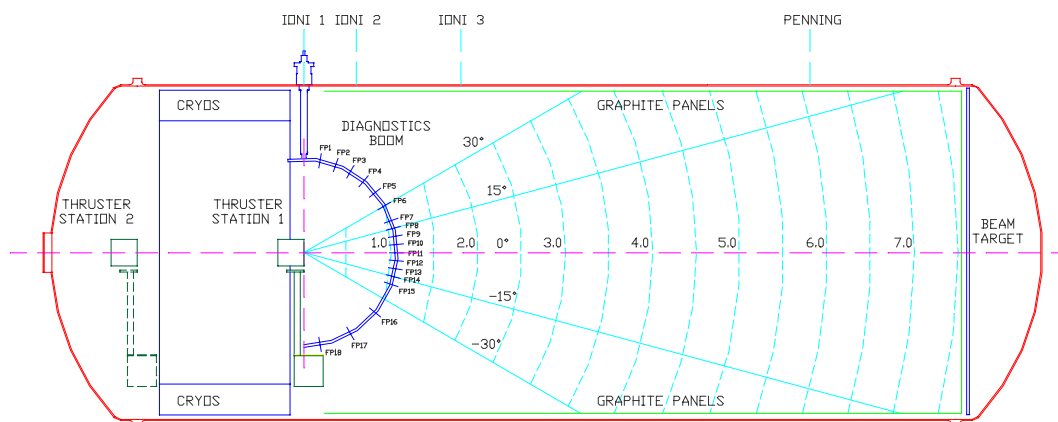

Fig. 3. The vacuum test facility.

4. VACUUM PERFORMANCE

Fig. 4 shows the vacuum behaviour during a typical pumpdown phase measured with the high vacuum gauges described in Par. 1. The subsequent pumps switching on can be recognised.
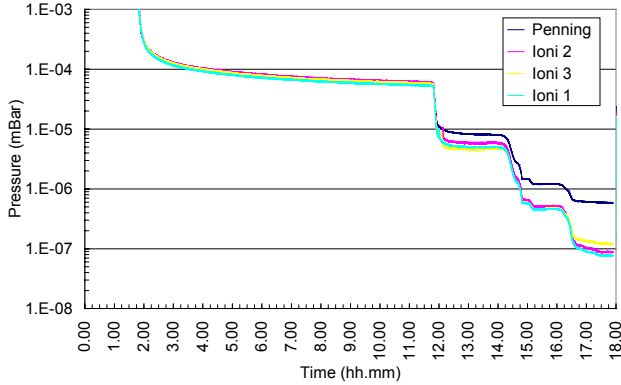

Fig. 4. Static vacuum.

Usually, the static vacuum of 1×10^{-7} mbar is obtained after 16 h pumping. After 72 h pumping the following vacuum data were obtained:

	Ioni 1	Ioni 2	Ioni 3	Penning
Static Vacuum (mbar)	6.2×10^{-8}	6.7×10^{-8}	1.2×10^{-7}	4.0×10^{-7}

The measured leak rate is 4.2×10^{-3} mbar l/s without test apparatus installed and 5.6×10^{-3} mbar l/s under thruster test conditions.

A cold flow test has been carried out introducing Xenon in the chamber through a Digital Mass Flow Controller (accuracy ±0.5% of the readings plus ±0.2% of the full scale). The Xenon flow rates of 12.5, 25, 37.5, 50, 37.5, 25, 12.5 sccm were sent in succession. Pressure readings are taken by the DAS and then scaled up using the Xenon correction factor 2.87. Note that in Fig. 5 the pressures are uncorrected.

Tab. 2 compares the dynamic vacuum measured at different distances from the thruster for the above Xenon flow rates. Pressure data are corrected for Xenon.

Tab. 2. Dynamic vacuum (cold flow test).

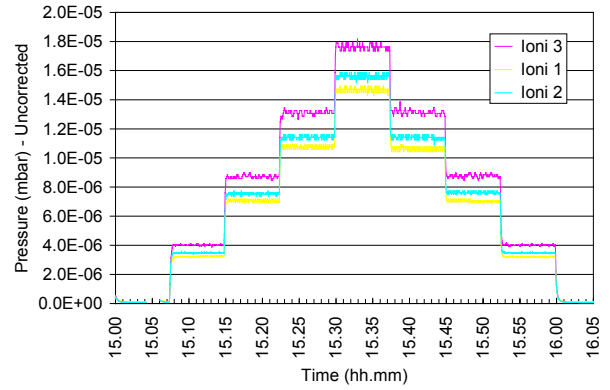| Flow Rate (sccm)	Ioni 1 (mbar)	Ioni 2 (mbar)	Ioni 3 (mbar)	Penning (mbar)
12.5	1.1×10^{-6}	1.2×10^{-6}	1.4×10^{-6}	1.9×10^{-6}
25	2.5×10^{-6}	2.6×10^{-6}	3.0×10^{-6}	4.0×10^{-6}
37.5	3.7×10^{-6}	4.0×10^{-6}	4.6×10^{-6}	5.7×10^{-6}
50	5.1×10^{-6}	5.4×10^{-6}	6.1×10^{-6}	7.6×10^{-6}

Fig. 5. Dynamic vacuum (cold flow test).

Therefore, the cold flow tests point out a pumping speed on Xenon from 215.000 l/s (@ 12.5 sccm) to 185.000 l/s (@ 50 sccm) at thruster exit section with a Xenon thermalisation temperature of 300 K.

Fig. 6 shows dynamic vacuum data obtained during a thruster firing test at different Xenon flow rates with the error bars.
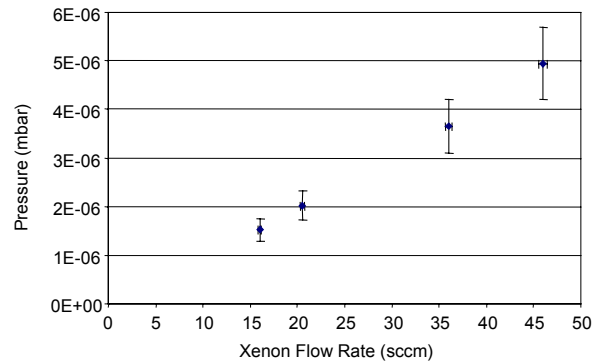

Fig. 6. Dynamic vacuum (thruster firing test).

The vacuum data show a pumping speed on Xenon from 198.000 l/s (@ 16 sccm) to 175.000 l/s (@ 46 sccm) at the thruster exit section, during thruster firing operations.

5. BEAM DIAGNOSTICS

The diagnostics set mounted on the rotating boom inside the chamber (Fig. 7) includes:
- 18 Faraday Probe (FP) with guard ring placed at different angular positions on the boom;
- 1 nude Faraday Probe (FPN) without guard ring mounted on a horizontal bar fixed on the boom in perpendicular direction of the thruster firing axis;
- 2 Retarding Potential Analyser (RPA) mounted on the same bar as FPN.

3

Fig. 7. FPs and RPAs on the diagnostics boom.

5.1 Faraday Probes

FPs are used for ion current density measurements. The ion density data are then elaborated to calculate the total beam current of the thruster, the divergence half angle and the deviation of the thrust vector.

The main problems usually encountered in the design of a Faraday probe are [2, 3, 4, 5]:
- repelling electrons in order to collect only the ion current without substantial sheat growth;
- collecting a higher current due to the edge effect;
- overestimation of the total beam current due to:
  - the effect of low energy charge exchange (CEX) ions;
  - the use of not suitable materials;
  - the effect of multiple charged ions.

Considering these questions, the adopted configuration is that designed by Myers et al. at NASA Le.R.C. [2, 6] including a collector and a guard ring. The probes are designed to be effective also for plasmas with Debye length greater than 0.04 mm.

Fig. 8 shows the electrical schematic of the FP: the ratio between the measured voltage V and the known resistance R_S is the collected ion current that must be divided by the collector area to obtain the ion current density.
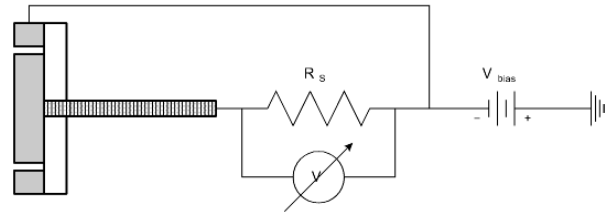

Fig. 8. Electric schematic of the Faraday probe.

Experiments have been performed rotating the boom while an electric thruster placed at station 1 was firing. Fig. 9 shows current density data acquired by the probe on the horizontal plane crossing the thruster axis. It is possible to note that the data acquired during the forward boom scan (blue 'x' points) are consistent with data from the subsequent backward scan (red '+' points).

Fig. 10 shows a 3D map of the current densities in the plume obtained by interpolating the probe data in α and in β (angular position of the boom and angular position of a probe on the boom respectively) and the related contour map.
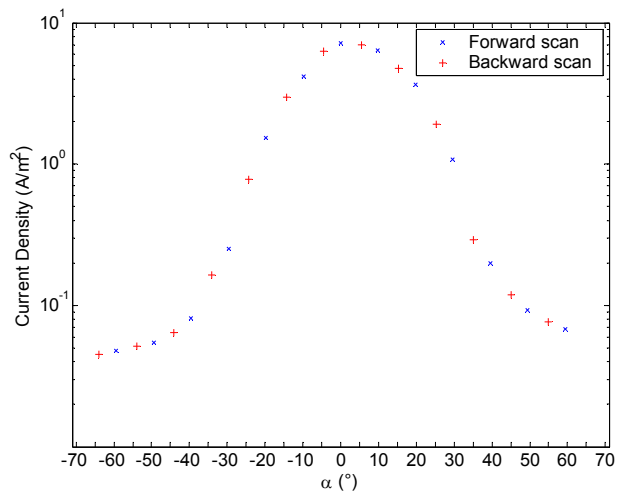

Fig. 9. Data from the probe crossing the thruster axis.

5.2 Retarding Potential Analysers

RPAs are used for ion energy measurements.
A RPA selectively filters out ions by applying a retarding potential across an inlet grid. The probe acts as a high-pass filter by allowing only ions with voltages (energy to charge ratios, $V = E/q$) greater than the grid voltage to pass and reach a collection electrode (collector). So the yielded ion current varies as a function of the ion retarding electrode potential.
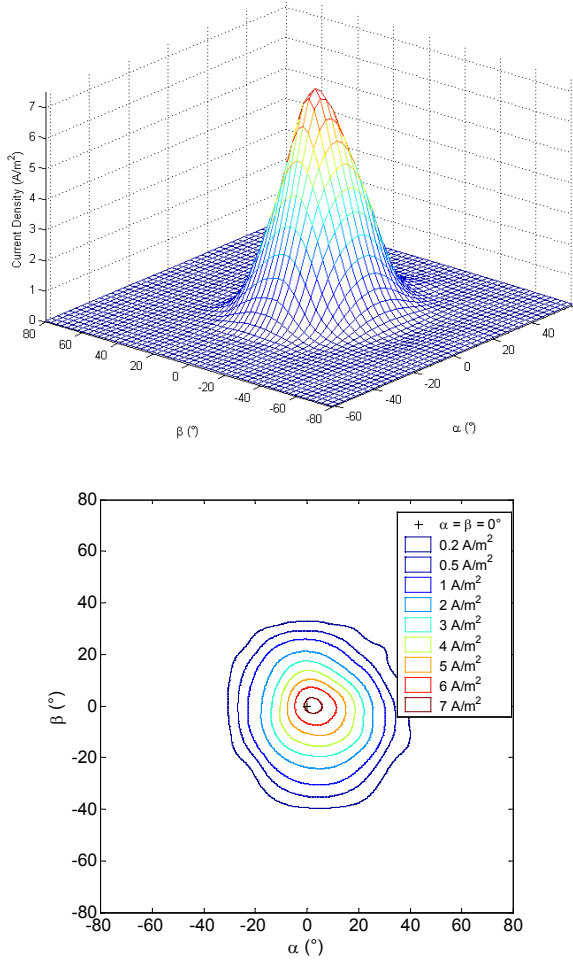
4

Fig. 10. 3D and contour map of current densities in the plume 1 m from the thruster exit.

The derivative of the resulting ion current-voltage characteristic (*dI/dV*) is proportional to the ion voltage distribution function *f(V)*) given by:

$$\frac{dI}{dV} = -\frac{q_i^2 e^2 n_i^2 A}{m_i} f(V) \qquad (1)$$

where q_i is the charge state of the ion, *e* is the elementary charge, n_i is the ion density, *A* is the probe collection area, and m_i is the ion mass. Under the assumption that the plasma is composed of ions of the same mass and charge, *f(V)* is identical to the ion energy distribution function.

The main problems usually encountered in the design of a RPA are [6, 7, 8]:
- repelling electrons in order to collect only the ion current without substantial sheath growth;
- artificial rise of the ion energy distribution because of Debye shielding;
- space charge limitations of energy analysers;
- discharges between too much closer grids;
- overestimation of the ion current due to the use of a not suitable materials;

Considering these questions, the adopted configuration includes three grids, a collector and a metallic outer body grounded to the vacuum facility. The probes are designed to be effective also for plasmas with Debye length greater than 0.04 mm.

During operation, the first grid is electrically isolated from the probe and facility ground to minimise disturbance to the ambient plasma from the strong electric fields generated within the probe. The second grid is biased to a constant negative potential of sufficient strength to repel all plasma electrons from the collector. The third one (the ion retarding grid) is connected to a variable high voltage power supply (0 ÷ 3000 V) . The ion current to the collector is measured by using a shunt calibrated resistor (0.1% accuracy) and a digital 2 channels oscilloscope *Agilent 54622*. Fig. 11 shows the electrical schematic of the RPA.
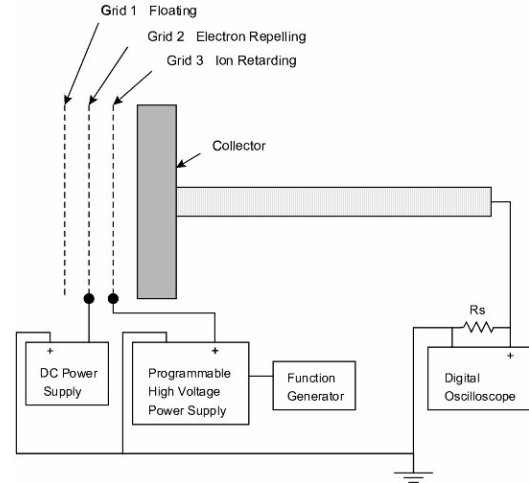

Fig. 11. Electric schematic of the RPA probe.

6. EMC LVTF CHARACTERIZATION

In the development of electric thrusters intended for space applications, any phenomena which may adversely affect a host spacecraft is deeply investigated, in particular, the thruster electromagnetic (EM) emissions.

The preliminary step necessary for a thruster EMI characterisation campaign is evaluating the EMC characteristics of the test site.

Thus, AEROSPAZIO performed a series of tests to:
- evaluate the electromagnetic (EM) environment inside the LVTF, i.e. characterise the EM signals either from broadcast or emitted by the facility equipment (pumps, probes, data acquisition systems, etc.);

5

- evaluate the EM shield level presented by the chamber case.

This investigation allows to find the base information needed for a shielding and/or filtering system.

The frequency range of interest is 100 kHz ÷ 22 GHz.

Tab. 3 lists the antennas used to cover this range, the associated bandwidth and polarisation.

Tab. 3. Antennas used for the EMC LVTF tests.

Frequency Range	Antenna Type	Polarisation
100 kHz ÷30 MHz	Stylus-Conical	Vertical
100 kHz ÷ 30 MHz	Active-Loop EMCO6507	Vertical
30 ÷ 300 MHz	Bi-Conical EM 6912A	Vertical
300 MHz ÷ 3 GHz	Log-Periodical EM 6952	Vertical
3 ÷ 22 GHz	Log-Periodical EM 6950	Vertical

The antennas are placed at the thruster station 1 inside the chamber and on the platform beside the chamber near to the data acquisition and control systems.

The outputs from the antennas were fed to a receiver system consisting of:
- a *PMM 8053* EM fields meter;
- a *PMM EP330* radiofrequency EM fields isotropic probe operating from 100 kHz to 3 GHz;
- a *Hewlett Packard HP8560A* spectrum analyser operating from 50 Hz to 2.9 (3) GHz;
- a *Hewlett Packard HP8569A* spectrum analyser operating from 40 MHz to 22 GHz.

The test programme started with an investigation of the background noise, detected over the complete frequency range of interest. Then, the EM signals in the same frequency range have been measured when all the facility equipment was switched on.

As examples, Fig. 12 shows the magnetic field in the range 100 KHz ÷ 30 MHz and Fig. 13 the electric field measured in the range 30 MHz ÷ 300 MHz. Both figures refers to data acquired from antennas placed inside the chamber when all the facility equipment was switched on.

7. REFERENCES

1. Bonelli E., *Sistema di acquisizione dati per prove in camera a vuoto di propulsori elettrici satellitari*, Master Thesis, University of Siena, 2003.

2. Walker L. R., et al., The effects of nude Faraday probe design and vacuum facility backpressure on the measured ion current density profile of Hall thruster plumes, AIAA-2002-4253, *Proc. of the 38th Joint Propulsion Conference*, Indianapolis, IN, 2002.
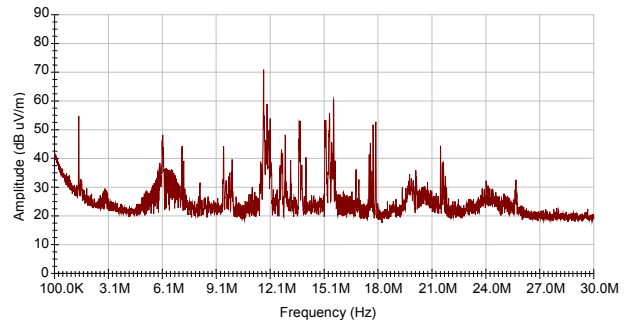
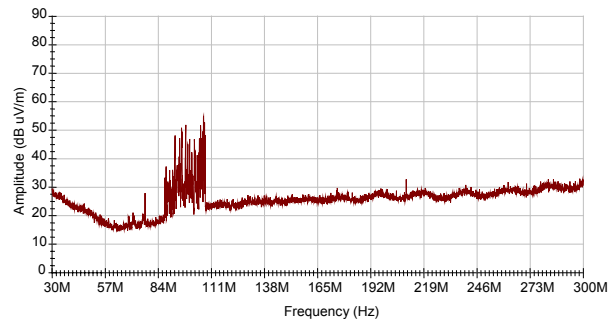Fig. 12. Magnetic field in the range 100 KHz ÷ 30 MHz. All equipment on. Antennas at station 1.

Fig. 13. Electric field in the range 30 MHz ÷ 300 MHz. All equipment on. Antennas at station 1.

3. Manzella D. H. and Sankovic J. M., Hall thruster ion beam characterisation, AIAA-95-2927, *Proc. of the 31st Joint Propulsion Conference*, San Diego, CA, 1995.

4. Haas J. M., *Low perturbation interrogation of the internal and near field plasma structure of a Hall thruster using a high speed probe positioning system*, Ph.D. Thesis, University of Michigan, 2001.

5. Hofer R. R., et al., A comparison of nude and collimated Faraday probes for use with Hall thruster, IEPC-01-020, *Proc. of the 27th International Electric Propulsion Conference*, Pasadena, CA, 2001.

6. Myers R. M. and Manzella D. H., Stationary plasma thruster plume characteristics, IEPC-93-096, *Proc. of the 23rd International Electric Propulsion Conference*, Seattle, 1993.

7. Marrese C. M., et al., Development of a Single-orefice Retarding Potential Analyzer for Hall Thruster Plume Characterization, IEPC-97-066, *Proc. of the 25th International Electric Propulsion Conference*, Cleveland, 1997.

8. Hofer R. R, et al., Ion voltage diagnostic in the far field plume of a high specific impulse Hall thruster, AIAA-2003-4556, *Proc. of the 39th Joint Propulsion Conference & Exhibit*, Huntsville, Alabama, 2003.